AD-A050 093 NAVAL RESEARCH LAB WASHINGTON D C F/G 20/9
IONIZATION EQUILIBRIUM AND RADIATIVE ENERGY LOSS RATES FOR C, N--ETC(U)
NOV 77 V L JACOBS, J DAVIS, J E ROGERSON

UNCLASSIFIED NRL-MR-3572 SBIE-AD-E000 088 NL

| OF |
AD
A050093

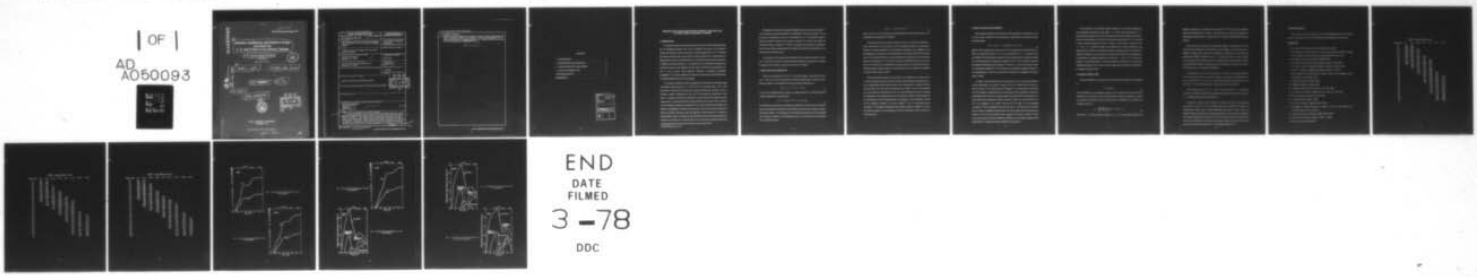

END
DATE
FILMED
3-78
DDC

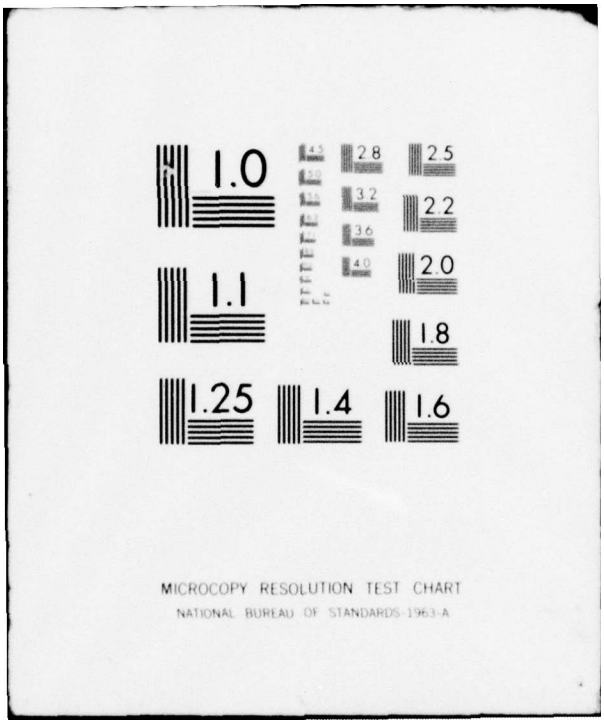
1.0
1.1
1.25
1.4
1.6
2.8
3.2
3.6
4.0
2.5
2.2
2.0
1.8
MICROCOPY RESOLUTION TEST CHART
NATIONAL BUREAU OF STANDARDS-1963-A

ADE000088

NRL Memorandum Report 3572

Ionization Equilibrium and Radiative Energy Loss Rates for C, N, and O Ions in Low-Density Plasmas

V. L. Jacobs, J. Davis, J. E. Rogerson and M. Blaha

Plasma Physics Division

Interim rept.,

NRL-MR-3572

Nov 77

17p.

SBIE

AD-E000 088

NAVAL RESEARCH LABORATORY
Washington, D.C.

251 950

SECURITY CLASSIFICATION OF THIS PAGE (When Data Entered)

REPORT DOCUMENTATION PAGE

READ INSTRUCTIONS BEFORE COMPLETING FORM

1. REPORT NUMBER: NRL Memorandum Report 3572
2. GOVT ACCESSION NO.
3. RECIPIENT'S CATALOG NUMBER

4. TITLE (and Subtitle): IONIZATION EQUILIBRIUM AND RADIATIVE ENERGY LOSS RATES FOR C, N, AND O IONS IN LOW-DENSITY PLASMAS
5. TYPE OF REPORT & PERIOD COVERED: Interim report on a continuing NRL Problem
6. PERFORMING ORG. REPORT NUMBER

7. AUTHOR(s): V.L. Jacobs, J. Davis, J.E. Rogerson, NRL, and M. Blaha, University of Maryland

8. CONTRACT OR GRANT NUMBER(s)

9. PERFORMING ORGANIZATION NAME AND ADDRESS: Naval Research Laboratory, Washington, D.C. 20375

10. PROGRAM ELEMENT, PROJECT, TASK AREA & WORK UNIT NUMBERS: 47A01-24B

11. CONTROLLING OFFICE NAME AND ADDRESS: National Aeronautics and Space Administration, Washington, D.C. 20545

12. REPORT DATE: November 1977

13. NUMBER OF PAGES: 16

14. MONITORING AGENCY NAME & ADDRESS(if different from Controlling Office)

15. SECURITY CLASS. (of this report): Unclassified

15a. DECLASSIFICATION/DOWNGRADING SCHEDULE

16. DISTRIBUTION STATEMENT (of this Report)

Approved for public release; distribution unlimited.

17. DISTRIBUTION STATEMENT (of the abstract entered in Block 20, if different from Report)

18. SUPPLEMENTARY NOTES

19. KEY WORDS (Continue on reverse side if necessary and identify by block number)

Dielectronic Recombination
Ionization Equilibrium
Charge State
Radiative Energy Loss

20. ABSTRACT (Continue on reverse side if necessary and identify by block number)

The results of calculations of the ionization equilibrium and radiative energy loss rates for C, N, and O ions in low-density plasmas are presented for electron temperatures in the range 10^4 - 10^7 K (~1 - 10^3 eV). The ionization structure is determined using the steady-state corona model, in which electron impact ionization from the ground states is balanced by direct radiative and dielectronic recombination. Using an improved theory, detailed calculations are carried out for the dielectronic recombination rates in which account is taken of all radiative and autoionization processes involving a single-electron electric-dipole transition of the recombining ion. The radiative

(Continued)

DD FORM 1 JAN 73 1473 EDITION OF 1 NOV 65 IS OBSOLETE
S/N 0102-LF-014-6601

SECURITY CLASSIFICATION OF THIS PAGE (When Data Entered)

20. ABSTRACT (Continued)

energy loss processes considered are electron-impact excitation of resonance line emission, direct radiative recombination, dielectronic recombination, and electron-ion bremsstrahlung. For all three elements, resonance line emission resulting from 2s - 2p transitions produces a broad maximum in the energy loss rate near 10^5 °K (≃ 10 eV).

100,000 K (about

CONTENTS

IONIZATION EQUILIBRIUM AND RADIATIVE ENERGY LOSS RATES FOR C, N, AND O IONS IN LOW-DENSITY PLASMAS

1. INTRODUCTION

An important method of determining the physical properties of high-temperature laboratory and astrophysical plasmas, such as their temperature and density, is the analysis of optically-thin spectral line intensities emitted by multiply-charged atomic ions.[1,2] In addition the presence of relatively small concentrations of multiply-charged ions in a predominantly hydrogen plasma can have an important effect on the collisional transport processes, such as particle diffusion and thermal conduction. It is well-known that the resonance line radiation from incompletely ionized ions can influence the power balance in laboratory and astrophysical plasmas as well as provide useful diagnostic information. Accordingly, spectroscopic investigations[3,4] have been conducted to determine the concentration and spatial distribution of multiply-charged impurity ions in such plasmas.

In this paper we present the results of calculations of the distribution of ionization stages and radiative energy loss rates for *C*, *N*, and *O* ions in a low-density plasma. Only a brief description of the methods will be given, since they have already been discussed in detail in previously reported investigations for Fe ions.[5,6] The steady-state optically-thin corona model[7] is applied to determine the distribution of ions of a given element among the various charge states. It is assumed that electron impact ionization from the ground states is balanced by direct radiative and dielectric recombination. The ionization equilibrium distributions thus obtained are independent of density and are functions of only the local electron temperature. Since the low-lying excited states which are produced by electron impact can be assumed to undergo radiative decay in times that are short compared with the time between collisions, the emission line intensities can be computed from the corona ionization equilibrium distributions of the ground states and the ground state electron impact excitation rates.

*Manuscript submitted July 20, 1977.

The essential innovation in the present investigation is the use of an improved theory [5] in the calculation of the rates for dielectronic recombination, which has been shown [8] to be the dominant recombination process for non-hydrogenic ions in the temperature region of maximum equilibrium abundance and maximum resonance line emission. The simple, and widely-used, formula of Burgess [9] is found to overestimate the dielectronic recombination rates for certain ionization stages because of the neglect of the effects of autoionization into an excited-state of the recombining ion.

The calculation of the dielectronic recombination rates is discussed in Section 2. In Section 3 the results of the corona ionization equilibrium calculations are presented. The theoretical predictions for the radiative energy loss rates are given in Section 4.

2. DIELECTRONIC RECOMBINATION

Dielectronic recombination of an ion X^{+z} with residual charge z is the result of two transitions. The first is a radiationless capture of an electron accompanied by excitation of one of the bound electrons in the recombining ion to form a doubly-excited state j, nl.

$$X^{+z}(i) + e^- \rightarrow X^{+(z-1)}(j, nl). \tag{1}$$

The second is a stabilizing radiative transition to a single-excited state i, nl which lies below the ionization threshold of the recombined ion.

$$X^{+(z-1)}(j, nl) \rightarrow X^{+(z-1)}(i, nl) + \hbar\omega. \tag{2}$$

The dielectronic recombination rate is equal to the product of the capture rate and the branching ratio representing the probability that the doubly-excited state decays through the stabilizing radiative transition. After summation over all important excited states j of the recombining ion and quantum numbers nl of the recombining electron, the total dielectronic recombination rate is obtained in the form

$$R_d(z, i) = N_e\, N(z, i)\, \alpha_d(z, i), \tag{3}$$

where N_e and $N(z, i)$ are the electron and initial (ground) state ion densities and $\alpha_d(z, i)$ is the dielectronic recombination rate coefficient.

The branching ratio for the stabilizing radiative transition is obtained by dividing the radiative transition rate by the total decay rate for all spontaneous radiative and autoionization processes. In previous calculations for the dielectronic recombination rate coefficients, it has been assumed that autoionization occurs predominantly into the ground state of the recombining ion. For certain excited states j of the recombining ion, autoionization into a lower excited state can occur through a $\Delta n = 0$ transition with a greater probability than the inverse of transition (1). The inclusion of this additional autoionization process in the branching ratio for the stabilizing radiative transition produces a substantial reduction of the dielectronic recombination rates for certain ionization stages.

We have calculated the dielectronic recombination rate coefficients for the various ions of *C*, *N*, and *O*, taking into account all radiative transitions and autoionization processes which involve a single-electron electric-dipole transition of the recombining ion. Because of the fact that large values of the outer-electron principal quantum number n play the most important role in the dielectronic recombination of low-z ions, the autoionization rates can be obtained by extrapolation of the threshold partial wave cross sections for electron impact excitation of the recombining ion. With increasing density, the populations of the most important nl-levels will be significantly influenced by electron impacts [10] and by ion-produced electric microfields. [11] The effective recombination rate coefficient defined by equation (3) will become density-dependent. The investigation of this density-dependence will be the subject of a forthcoming paper.

3. CORONA IONIZATION EQUILIBRIUM

When transport processes and time-variations can be neglected, the distribution of ions of a given element among the various charge states is determined by the steady-state corona model relationships

$$N(z-1)S(z-1) = N(z)\alpha(z), 1 \leqslant z \leqslant Z, \tag{4}$$

together with the condition that the sum over all $N(z)$ correspond to the total abundance N_Z. Here $N(z)$ denotes the density of X^{+z} ions in the ground state. $S(z-1)$ denotes the total rate coefficient for electron impact ionization from the ground state and is obtained by adding to the semi-empirical direct ionization rate coefficient of Lotz [12] the contribution describing autoionization following inner-shell excitation. [13] Finally, $\alpha(z)$ is the sum of the direct radiative recombination coefficient [5] and the dielectronic recombination coefficient discussed in the preceeding section. Three-body recombination is estimated to the negligible in the density region of interest.

In Table 1-3 the relative abundances of the various ions of *C*, *N*, and *O* are presented for electron temperatures in the range $4.0 \leqslant \log_{10} T_e(°K) \leqslant 7.0$. Similar results have been reported by Jordan, [13] who used the formula of Burgess [9] for the dielectronic recombination rates. The inclusion of autoionization into an excited state of the recombining ion reduces the recombination rates for the lower ionization stages. This causes a shift of the maximum abundance toward lower temperatures. However, this shift is found to be less important for the low-z ions considered in the present work than for the high-z Fe ions investigated previously. [5,6] This is a consequence of the fact that the $2s - 2p$ transitions of the recombining ion, which are not affected by autoionization into an excited state, are found to be most important in the low-z ions. The present results, in agreement with those of Jordan, [13] predict that a given ion has its maximum equilibrium abundance at a much higher temperature than that obtained [14] without the inclusion of dielectronic recombination.

The contributions to the collisional transport coefficient [15] from multiply-charged ions can be estimated by knowing the mean charge $< z >$ and the mean square charge $< z^2 >$. The mean square charge also enters into the estimation of the radiative energy loss rate due to electron-ion bremsstrahlung. The mean and mean square charges obtained for *C*, *N*, and *O* ions in corona ionization equilibrium are shown in Figures 1-3 as functions of temperature. The $< z >$ and $< z^2 >$ curves show initially a rapid increase with T_e which is followed by a flat region where the *He*-like ion is predominant, because a substantial increase in temperature is required for ionization of a 1s electron from the closed shell. The effect of including dielectronic recombination is a substantial reduction in the values of $< z >$ and $< z^2 >$ at a given temperature. In the following section, it will become apparent that this shift of the ionization-recombination balance in favor of lower ionization stages tends to enhance the line radiation in an important temperature region.

4. RADIATIVE ENERGY LOSS

The power radiated per unit volume as a result of electron-ion collisions can be expressed as

$$P = N_e N_Z \epsilon_Z, \tag{5}$$

where the efficiency ϵ_Z is independent of density and is a function of only the local electron temperature. In corona equilibrium the dominant radiative energy loss mechanism is expected to be resonance line radiation excited by electron impact. The efficiency for this radiation loss mechanism is given by

$$\epsilon_Z = \sum_{z=1}^{Z-1} \frac{N(z)}{N_Z} \sum_j \Delta E(z, i \rightarrow j) C(z, i \rightarrow j), \tag{6}$$

where $\Delta E(z, i \rightarrow j)$ are the excitation energies, $C(z, i \rightarrow j)$ are the collisional excitation rate

coefficients obtained from a distorted wave calculation,[16] and $N(z)/N_Z$ are the ionization equilibrium distributions given in Tables 1-3. We have taken into account only single-electron electric-dipole transitions from the valence shell, and the effects of self-absorption have been neglected.

During the process of dielectronic recombination, radiation is emitted close to the resonance line of the recombining ion. The efficiency for this radiation can be calculated after replacing the electron impact excitation rate coefficient in Equation (6) by the dielectronic recombination coefficient associated with the $i \rightarrow j$ transition. We defer to a future investigation the calculation of the energy loss rate for the radiation which is emitted when the *nl*-states of the outer-electron cascade to the ground state of the recombined ion, because this contribution is expected to have a strong density-dependence.

The efficiencies for electron impact excitation of resonance line radiation, dielectronic recombination radiation, direct recombination radiation, and electron-ion bremsstrahlung are shown in Figures 4-6 for *C*, *N*, and *O* ions. Similar calculations have been carried out by Cox and Tucker,[17] but the individual radiative energy loss rates were not presented.

The brood maximum near 10^5 °*K* ($\sim$ 10 eV) is produced mainly by $2s - 2p$ transitions in the lower ionization stages, while the smaller peak at higher temperatures is the result of $1s - 2p$ transitions of the *He*-like and *H*-like ions.

Although the radiation emitted through the stabilizing transitions in the dielectronic recombination process can be more important than direct recombination radiation and bremsstrahlung, electron impact excitation of resonance line emission is clearly the dominant radiative energy loss mechanism for incompletely ionized ions. On the other hand, the shift of the ionization-recombination balance in favor of lower ionization stages which results from the inclusion of the dielectronic recombination rates tends to enhance the loss rate due to line radiation, which falls off approximately as $1/T_e$ at the higher temperatures.[18]

ACKNOWLEDGMENTS

This investigation has been supported by the NASA Headquarters and the E.O. Hulburt Center for Space Research, as part of the ATM Data Analysis Program funded by NASA.

REFERENCES

1. H.R. Griem, *Plasma Spectroscopy* (McGraw-Hill, New York, 1964).
2. A.H. Gabriel and C. Jordan, Chapter 4 in *Case Studies in Atomic Collision Physics II,* edited by E.W. McDaniel and M.R.C. McDowell (North Holland, New York, 1972).
3. W.H. Tucker and M. Koren, Astrophys. J. **168,** 283 (1971).
4. K.J.H. Phillips, W.M. Neupert, and R.J. Thomas, Solar phys. **36,** 383 (1974)).
5. V.L. Jacobs, J. Davis, P.C. Kepple, and M. Blaha, Astrophys. J., **211,** 605 (1977).
6. J. Davis, V.L. Jacobs, P.C. Kepple, and M. Blaha, J QSRT **17,** 139 (1977).
7. R.W.P. McWhirter in *Plasma Diagnostic Techniques,* edited by R.H. Huddleston and S.L. Leonard (New York, Academic, 1965).
8. A. Burgess, Astrophys. J. **139,** 776 (1964).
9. A. Burgess, Astrophys. J. **141** 1588 (1965).
10. A. Burgess and H.P. Summers, Astrophys. J. **157,** 1007 (1969).
11. V.L. Jacobs, J. Davis, and P.C. Kepple, Phys. Rev. Letters, **37,** 1390 (1976).
12. W. Lotz, Astrophys. J. Suppl. Serv. **14,** 207 (1967).
13. C. Jordan, N.N.R.A.S. **142,** 501 (1969).
14. L.L. House, Astrophys. J. Suppl. Serv. **8,** 307 (1964).
15. S.I. Braginskii, "Transport Processes in a Plasma," in *Reviews of Plasma Physics,* Vol. 1 (Consultants Bureau, New York, 1965).
16. J. Davis, P.C. Kepple, and M. Blaha, J QRST **16,** 1043 (1976).
17. D.P. Cox and W.H. Tucker, Astrophys. J. **157,** 1157 (1969).
18. H.R. Griem, private communication.

Table 1 — $\log_{10} N(z)/N_Z$ for *C* Ions

$\log_{10}T_e$ (°K)	C I	C II	C III	C IV	C V	C VI	C VII
4.0	0.13	0.56					
4.1	0.86	0.06					
4.2	1.66	0.01	4.07				
4.3	2.04	0.00	2.72				
4.4	2.18	0.01	1.80				
4.5	2.30	0.03	1.11				
4.6	2.50	0.12	0.61	4.54			
4.7	2.82	0.32	0.29	2.96			
4.8	3.26	0.61	0.13	1.77	4.09		
4.9	3.80	0.99	0.11	0.90	2.04		
5.0	4.61	1.63	0.39	0.46	0.63		
5.1		2.84	1.27	0.73	0.11		
5.2		4.22	2.34	1.29	0.02		
5.3			3.31	1.81	0.00		
5.4			4.15	2.26	0.00		
5.5			4.88	2.64	0.00	4.00	
5.6				2.97	0.00	2.61	
5.7				3.27	0.01	1.50	4.89
5.8				3.61	0.10	0.68	2.93
5.9				4.13	0.40	0.23	1.56
6.0				4.86	0.94	0.15	0.74
6.1					1.62	0.33	0.29
6.2					2.37	0.66	0.10
6.3					3.09	1.03	0.04
6.4					3.72	1.38	0.01
6.5					4.27	1.68	0.01
6.6					4.76	1.95	0.00
6.7						2.19	0.00
6.8						2.40	0.00
6.9						2.59	0.00
7.0						2.76	0.00

Table 2 — $\log_{10} N(z)/N_Z$ for N Ions

$\log_{10} T_e$ (°K)	N I	N II	N III	N IV	N V	N VI	N VII	N VIII
4.0	0.00	2.42						
4.1	0.05	0.90						
4.2	0.57	0.13						
4.3	1.43	0.01	3.77					
4.4	1.97	0.01	2.32					
4.5	2.17	0.02	1.34					
4.6	2.32	0.09	0.71	4.46				
4.7	2.59	0.26	0.33	3.02				
4.8	2.99	0.54	0.15	1.97				
4.9	3.47	0.89	0.09	1.18	4.28			
5.0	4.04	1.31	0.14	0.62	2.63			
5.1	4.75	1.84	0.35	0.29	1.41	2.72		
5.2		2.59	0.80	0.28	0.64	1.03		
5.3		3.85	1.79	0.85	0.59	0.22		
5.4			3.14	1.84	1.04	0.04		
5.5			4.41	2.78	1.53	0.01		
5.6				3.61	1.96	0.00		
5.7				4.33	2.33	0.00	3.57	
5.8				4.96	2.65	0.00	2.32	
5.9					2.95	0.02	1.33	4.21
6.0					3.30	0.12	0.60	2.50
6.1					3.82	0.42	0.23	1.32
6.2					4.52	0.94	0.19	0.61
6.3						1.59	0.38	0.25
6.4						2.28	0.69	0.10
6.5						2.92	1.02	0.04
6.6						3.50	1.33	0.02
6.7						4.01	1.60	0.01
6.8						4.47	1.85	0.00
6.9						4.48	2.06	0.00
7.0							2.26	0.00

Table 3 — $\log_{10} N(z)/N_Z$ for *O* Ions

$\log_{10}T_e$ (°K)	O I	O II	O III	O IV	O V	O VI	O VII	O VIII	O IX
4.0	0.02	1.28							
4.1	0.48	0.17							
4.2	1.56	0.01	7.50						
4.3	2.39	0.00	5.20						
4.4	2.80	0.00	3.45						
4.5	2.99	0.00	2.20						
4.6	3.14	0.02	1.32	5.43					
4.7	3.34	0.09	0.69	3.64					
4.8	3.66	0.30	0.30	2.33					
4.9	4.11	0.63	0.13	1.41	4.72				
5.0	4.66	1.06	0.13	0.76	3.10				
5.1		1.60	0.27	0.36	1.89	4.88			
5.2		2.25	0.58	0.19	1.03	2.99			
5.3		3.03	1.04	0.24	0.50	1.60	2.73		
5.4		4.04	1.76	0.59	0.34	0.72	1.02		
5.5			3.02	1.53	0.84	0.62	0.23		
5.6			4.61	2.82	1.75	1.01	0.05		
5.7				4.04	2.63	1.45	0.01		
5.8					3.40	1.85	0.01	4.22	
5.9					4.08	2.19	0.00	2.91	
6.0					4.66	2.48	0.01	1.88	
6.1						2.73	0.03	1.10	3.37
6.2						2.99	0.13	0.58	2.02
6.3						3.31	0.34	0.33	1.08
6.4						3.75	0.70	0.31	0.49
6.5						4.32	1.19	0.49	0.20
6.6						4.94	1.75	0.77	0.08
6.7							2.28	1.06	0.04
6.8							2.77	1.34	0.02
6.9							3.23	1.58	0.01
7.0							3.64	1.80	0.01

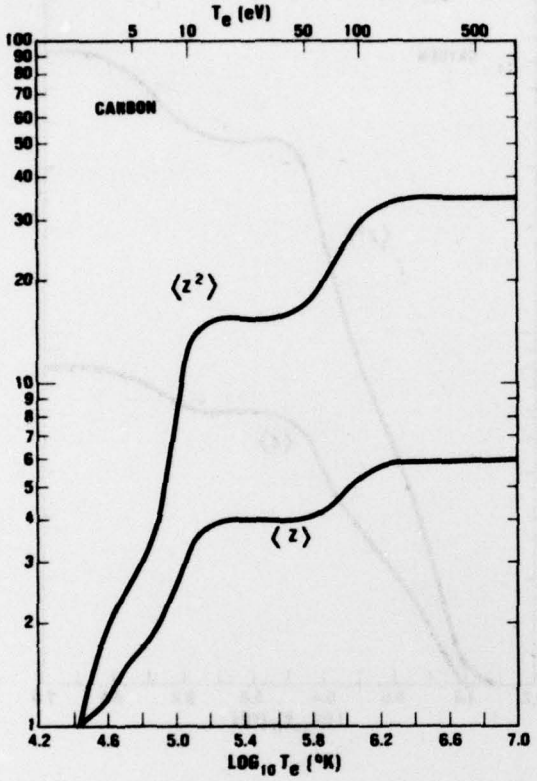

Fig. 1 — The mean and mean squared charges of C ions in corona equilibrium.

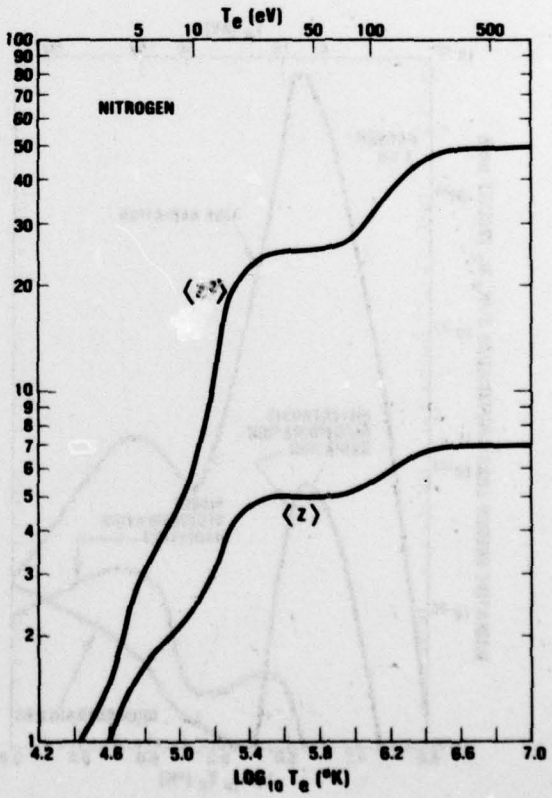

Fig. 2 – The mean and mean squared charges of N ions in corona equilibrium.

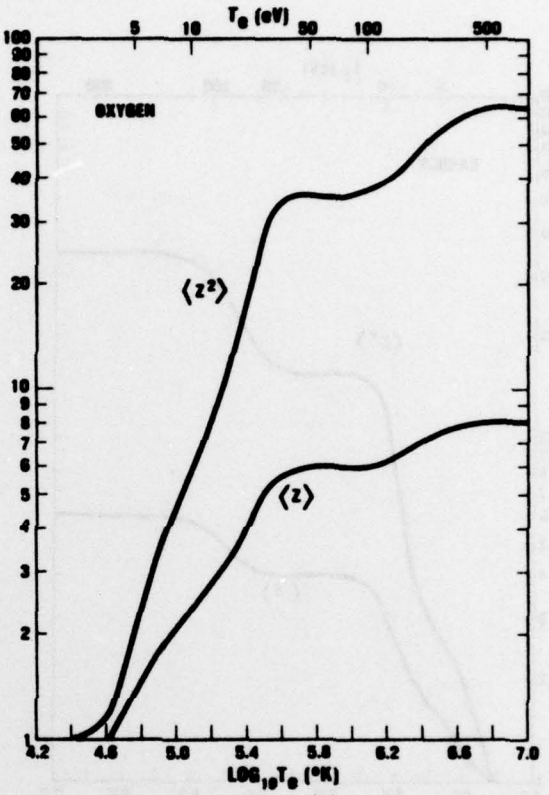

Fig. 3 – The mean and mean squared charges of O ions in corona equilibrium.

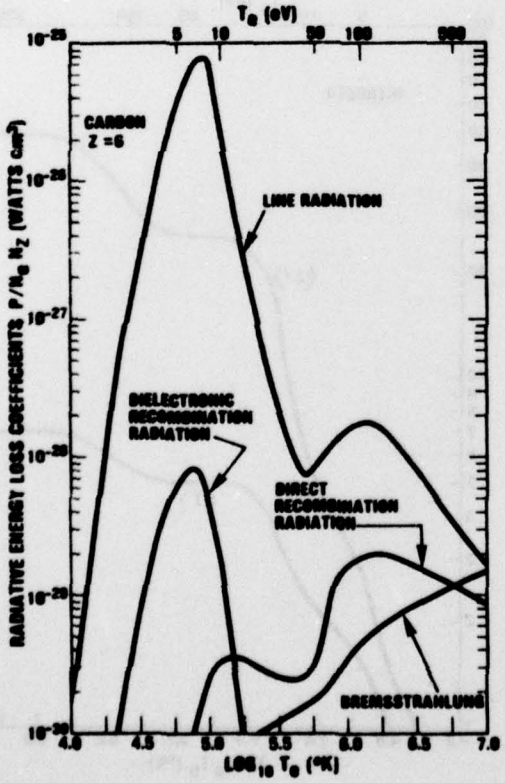

Fig. 4 – The radiative energy loss efficiencies for C ions in corona equilibrium.

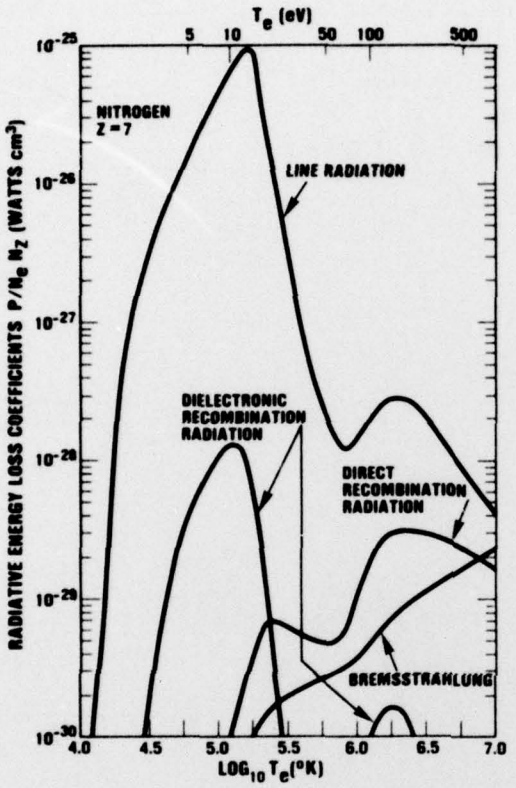

Fig. 5 – The radiative energy loss efficiencies for N ions in corona equilibrium.

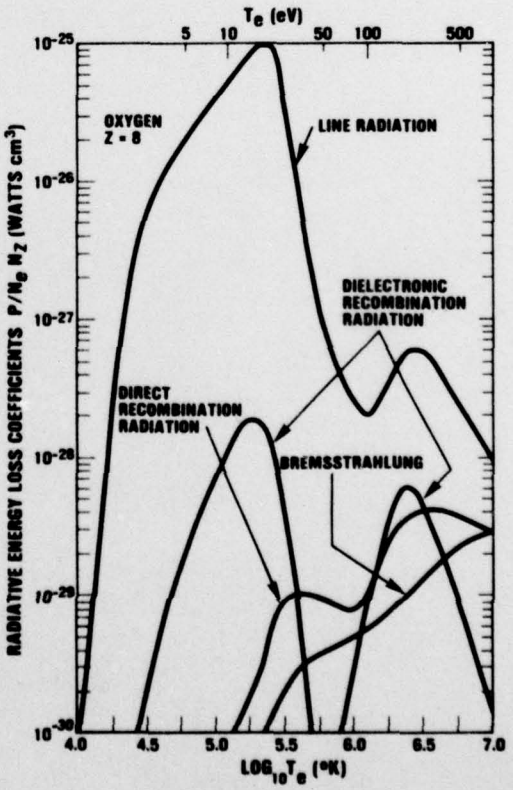

Fig. 6 – The radiative energy loss efficiencies for O ions in corona equilibrium.